

1 **Spatio-temporal assessment of annual water-balance model for Upper Ganga** 2 **Basin**

3 Anoop Kumar Shukla¹, Shray Pathak¹, Lalit Pal¹, Chandra Shekhar Prasad Ojha¹, Ana Mijic²,
4 Rahul Dev Garg¹

5 ¹Department of Civil Engineering, Indian Institute of Technology Roorkee, Uttarakhand, India

6 ²Department of Civil and Environmental Engineering, Imperial College London, London, UK

7 E-mail- anoopgeomatics@gmail.com, shraypathak@gmail.com, lalitpl4@gmail.com,
8 cspojha@gmail.com, ana.mijic@imperial.ac.uk, rdgarg@gmail.com

9 **Abstract**

10 The Upper Ganga Basin, Uttarakhand, India has high hydropower potential and plays an important
11 role in development of state economy. Thus, knowledge about water yield is of paramount
12 importance to this region. The paper deals with use of contemporary water yield estimation
13 models, such as the distributed model (InVEST), Lumped Zhang model and their validation to
14 identify the most suited one for water yield estimation in this region. Earlier, while utilizing these
15 models, water yield was estimated by considering a single value of some important model
16 parameters which in fact show distributed variation at finer (pixel) scale. Therefore, in this study,
17 pixel level computations are performed to assess and ascertain the need for incorporating spatial
18 variation of such parameters in model applications. To validate the findings, the observed sub-
19 basin discharge data is analyzed with the computed water yield for four decades, i.e. 1980, 1990,
20 2001 and 2015. The results obtained are in good agreement with the water yield obtained at pixel
21 scale.

22 **Keywords:** Ecosystem, Evapotranspiration, Water Yield, Lumped Zhang model, InVEST model

23 **1. Introduction**

24 Accurate assessment of key ecosystem services (ES) such as water yield have gained focus in
25 recent years in ES modelling as fresh water availability in a region are essential for agriculture,
26 industry, human consumption, hydropower, etc., (Readhead et al., 2016). Hydrological ecosystem
27 services generally include drinking water supply, power production, industrial use, irrigation, and
28 many more. Accurate estimation of water yield further facilitates in identification of hotspots for
29 stormwater harvesting in order to fulfill fresh water demand in the region (Pathak et al., 2017).
30 These hydrological ES are dependent on different factors such as watershed characteristics (e.g.
31 topography, land use land cover (LULC), soil type) and climatic condition. To incorporate these
32 concepts into assessment and decision making, there has been a proliferation of ecosystem
33 modelling tools and methods. Models for ES valuation often focus on using globally available
34 data, accepting large number of spatially explicit inputs and producing spatially explicit output,
35 and limiting the model structure to key biophysical processes involved in land-use change (Guswa
36 et al. 2014). Precise estimation of ES using these models is a complicated task owing to spatial
37 variability and dependence of ES on various topographical and climatic factors. Further, validation
38 and uncertainty assessment in model output have proven to be a key obstacle to the application of
39 ES models. In the literature, studies focusing on comparison of different ES models have projected
40 some light over the model output validation issues, however, there still exist lack of studies
41 highlighting validation of these models for Indian river basins. The benefits that can be derived
42 from ES should be analyzed and quantified in a spatially explicit manner (Sanchez et al. 2012).
43 The uncertainties in the determination of spatial and temporal distribution of the climatic variables,
44 especially precipitation, constitute a major obstacle to the understanding of hydrological behaviour
45 at the catchment scales (Milly et al. 2002).

46 The Integrated Valuation of ES and Tradeoffs (InVEST) model, developed by Natural Capital
47 Project (Tallis et al. 2010) is a tool which provides a framework to planners and decision makers
48 to assess trade-offs among ES and enables their comparison in various climate and land use change
49 scenarios. It includes a biophysical component which facilitates the provision of freshwater or
50 water yield by different parts of the landscape and a valuation component, representing the benefits
51 of water provisioning to people. The model works on simplified Budyko theory, which has a long
52 history and still continues to receive interest in the hydrological literature (Budyko 1979; Zhang
53 et al. 2001; Zhang et al. 2004; Ojha et al. 2008; Zhou et al. 2012; Donohue et al. 2012; Xu et al.
54 2013; Wang et al. 2014). The InVEST model applies a one-parameter formulation of the Budyko
55 theory in a semi-distributed manner (Zhang et al. 2004). The model is capable of quantifying the
56 water yield of a catchment under the influence of change in different drivers viz. climate variables
57 and catchment characteristics (e.g. land use change). Various studies have been carried out in the
58 past demonstrating the application of InVEST model to different river basins around the world.
59 Sanchez-Canales et al. (2012) carried out sensitivity analysis of three parameters i.e. z (seasonal
60 precipitation coefficient), precipitation (annual) and ET_0 (annual reference evapotranspiration)
61 using the InVEST model for a Mediterranean basin and found precipitation to be the most sensitive
62 parameter for the study region. Later, Terrado et al. (2014) applied the InVEST model for heavily
63 humanized Llobregat river basin. The model is applied for both extreme wet and dry conditions
64 and the role of climatic parameters is emphasized. Hoyer et al. (2014), applied this model in
65 Tualatin and Yamhill basins of northwestern Oregon under a series of urbanization and climate
66 change scenarios. The results show that the climatic parameters have more sensitivity than other
67 inputs for a water yield model. Hamel et al. (2014), applied the same water yield model for the
68 Cape Fear catchment, North Carolina and concluded that the precipitation is the most influencing

69 parameter. Goyal et al. (2017) analyzed the InVEST water yield model for the hilly catchment by
70 considering two catchments i.e. Sutlej river catchment and Tungabhadra river catchment. The
71 climate parameters i.e. precipitation and ET_0 are observed to be most influencing parameters for
72 water yield in both the river basins. With the aforementioned studies, there exist certain factors
73 limiting the application of InVEST model such as the absence or inadequate comparison with
74 observed data, calibration of the model without prior identification of sensitive parameters, and
75 lack of validation of the predictive capabilities in the context of Land Use Land Cover change (Bai
76 et al. 2012; Nelson et al. 2010; Su et al. 2013; Terrado et al. 2014).

77 The InVEST model operates on the principle of Budyko theory (Budyko, 1958, 1974). Based on
78 works of Schreiber (1904) and Ol'Dekop (1911), Budyko proposed formulations explaining the
79 relationship between precipitation and potential evapotranspiration (PET) in order to couple water
80 and energy balances, defined as Budyko hypothesis. Several attempts have been made later to
81 obtain an analytical solution of the Budyko hypothesis (Schreiber, 1904; Ol'Dekop, 1911; Turc,
82 1954; Mezentsev, 1955; Pike, 1964; Fu, 1981; Choudhury, 1999; Zhang et al., 2001, 2004;
83 Porporato et al., 2004; Yang et al., 2008; Donohue et al., 2012; Wang and Tang, 2014; Zhou et al.,
84 2015). Among these approaches, solutions provided by Fu (1981), called Fu's equation gained
85 significant attention as the work represented the effect of catchment properties on water balance
86 components by incorporating an addition parameter 'w'. Fu's equation can provide a full picture
87 of the evaporation mechanism at the annual timescale. Therefore, Fu's equation could be used
88 through top-down analysis for providing an insight into the dynamic interactions among climate,
89 soils, and vegetation and their controls on the annual water balance at the regional scale (Yang et
90 al., 2007).

91 Considering the lack of studies on analysis and validation of ES in Indian sub-continent especially
92 for Himalayan catchments and to assess the applicability of various water-balance model to
93 Himalayan catchments, the present work attempts to compute and analyse water yield in Upper
94 Ganga basin using InVEST model. The work primarily considers in detail, the spatial variation of
95 InVEST model parameters and uses different strategies to compute water yield. Accordingly,
96 water yield is estimated for four years i.e. 1980, 1990, 2001 and 2015 and the most appropriate
97 strategy is identified. The parameters that are computed at basin level scale in previous studies are
98 estimated at pixel scale in order to avoid the dependence of model parameters on size of the
99 catchment. In addition, pixel level estimations of water yield are expected to be more accurate than
100 output obtained using conventional approach. The term ‘finer scale’ in the paper represents the
101 incorporation of spatial variations through pixel level estimation of parameters involved in
102 InVEST model which are otherwise taken as lumped. The work also attempts to compare the
103 outcomes of spatially distributed water yield model and conventionally used lumped Zhang model.

104 **2. Background Theory**

105 ***2.1 Water Yield Models***

106 In this section, two water yield models, i.e. InVEST water yield model, which is a distributed
107 model and Lumped Zhang model are described.

108 ***2.1.1 InVEST model***

109 The InVEST water yield model (Tallis *et al.* 2010) is designed to provide the information regarding
110 the changes in the ecosystem that are likely to alter the flow. It is based upon the Budyko theory
111 which is an empirical function that yields the ratio of actual to potential evapotranspiration (PET)
112 (Budyko, 1979). To describe the degree to which long-term catchment water-balance deviates

113 from the theoretical limits, number of scholars have proposed one-parameter functions that can
114 replicate the Budyko curve (Fu 1981, Choudhury 1999, Zhang et al. 2004, Wang et al. 2014). To
115 observe and represent pixel-level changes to the landscape, InVEST model incorporates,
116 explicitly, the spatial variability in precipitation, PET, soil depth and vegetation. The model
117 operates at grid scale and acquire the inputs in raster format into a GIS environment such as
118 ArcGIS.

119 The InVEST water yield model is based on an empirical function known as the Budyko curve
120 (Budyko 1974). Annual Water yield, $Y(x)$ is determined for each pixel for a landscape as follows:

$$121 \quad Y(x) = \left(1 - \frac{AET(x)}{P(x)}\right) \times P(x) \quad (1)$$

122 where, $AET(x)$ is the actual annual evapotranspiration per pixel x ; and $P(x)$ is the annual
123 precipitation per pixel x . Actual evapotranspiration (AET) is essentially determined by climate
124 factors (precipitation, temperature, etc.) and mediated by catchment characteristics (vegetation
125 cover, soil characteristics, topography, etc.). On the other hand, potential evapotranspiration (PET)
126 represents the evaporating potential of the climate system at a specific location and time of year
127 without the consideration of catchment characteristics and soil properties (Allen et al., 1998).
128 Several attempts have been made in past to establish a relationship between AET and PET among
129 which solution provided by Fu (1981) is adopted worldwide. Fu (1981) provided an analytical
130 solution to the Budyko hypothesis and related AET with PET by incorporating a dimensionless
131 parameter 'w' which denotes the effect of catchment characteristics.

132 The InVEST model uses the expression of the Budyko curve proposed by Fu (1981) and Zhang *et*
133 *al.* (2004). The ratio of mean annual PET to annual precipitation, known as index of dryness, is
134 expressed as:

135
$$\frac{AET(x)}{P(x)} = 1 + \frac{PET(x)}{P(x)} - \left[1 + \frac{PET(x)}{P(x)} \right]^{\left(\frac{1}{\omega}\right)} \quad (2)$$

136 where, $PET(x)$ is the annual potential evapotranspiration per pixel x (mm); and $w(x)$ is a non-
 137 physical parameter that influences the natural soil properties. The $PET(x)$ is calculated using the
 138 following expression:

139
$$PET(x) = Kc(x) \times ETo(x) \quad (3)$$

140 where, $ETo(x)$ is the annual reference evapotranspiration per pixel x which is computed based
 141 on evapotranspiration from grass of alfalfa grown at that location using equation (6). $Kc(x)$ is the
 142 vegetation evapotranspiration coefficient that is influenced by the change in characteristics of land
 143 use land cover at every pixel (Allen et al., 1998). The values of $ETo(x)$ are adjusted by $Kc(x)$
 144 for each pixel over the land use land cover map. $w(x)$ is an empirical parameter and the expression
 145 given by Donohue et al. (2012) for the InVEST model has been applied to define $w(x)$ which is
 146 as follows:

147
$$w(x) = z \times \frac{AWC(x)}{P(x)} + 1.25 \quad (4)$$

148 Thus, the minimum value of the parameter $w(x)$ is 1.25 corresponding to bare soil where root
 149 depth is zero (Donohue et al. 2012) . The Donohue model was originally developed for Australia,
 150 however, the online documentation on InVEST model states its application globally. The
 151 parameter, z is known as seasonality factor whose value varies from 1 to 30. It represents the nature
 152 of local precipitation and other hydrogeological parameters. The parameter, $AWC(x)$ depicts
 153 volumetric plant available water content expressed in depth (mm) which can be expressed by
 154 following formula for each pixel x :

155
$$AWC(x) = Min. (Restricting\ layer\ depth, root\ depth) \times PAWC \quad (5)$$

156 Root restricting layer depth is defined as the depth of the soil upto which the soil can allow the
 157 penetration of roots and root depth is defined as the depth where 95 percent of the root biomass
 158 occurs. Plant Available Water Content (PAWC) is generally taken as the difference between the
 159 field capacity and wilting point. It depends upon the soil properties and can be computed by the
 160 Soil-Plant-Air-Water (SPA-W) software. PAWC is calculated using the method described by
 161 Mckenzie et al. (2003). Modified Hargreaves method and Hargreaves method were employed for
 162 computing the reference evapotranspiration for the study area at pixel scale.

163 Modified Hargreaves method

$$164 \quad ET_o = 0.0013 \times 0.408 \times RA \times (T_{avg} + 17.0) \times (TD - 0.0123 \times P)^{0.76} \quad (6)$$

165 where, ET_o is reference evapotranspiration, T_{avg} is average daily temperature ($^{\circ}C$) defined as the
 166 average of mean daily maximum and mean daily minimum temperature, TD ($^{\circ}C$) is the temperature
 167 range computed as the difference between mean daily maximum and mean daily minimum
 168 temperature, and RA is extraterrestrial radiation expressed in [$MJm^{-2}d^{-1}$].

169 Hargreaves method

$$170 \quad ET_o = 0.0023 \times 0.408 \times RA \times (T_{avg} + 17.8) \times TD^{0.5} \quad (7)$$

171 where, ET_o is reference evapotranspiration, T_{avg} is average daily temperature ($^{\circ}C$) defined as the
 172 average of mean daily maximum and mean daily minimum temperature, TD ($^{\circ}C$) is the temperature
 173 range computed as the difference between mean daily maximum and mean daily minimum
 174 temperature, and RA is extraterrestrial radiation expressed in ($MJm^{-2}d^{-1}$).

175 For computing the extraterrestrial radiation (RA), following equation is used

$$176 \quad RA = \frac{24(60)}{\pi} \times G_{sc} \times d_r \times [w_s \sin(\varphi) \sin(\delta) + \cos(\varphi) \cos(\delta) \sin(w_s)] \quad (8)$$

177 where, RA is extraterrestrial radiation [$MJm^{-2}d^{-1}$], d_r is the inverse relative distance Earth-Sun, G_{sc}
178 is solar constant equals to $0.0820 MJm^{-2}min^{-1}$, w_s is sunset hour angle (rad), δ is solar declination
179 (rad) and φ is latitude (rad).

180 *Determination of Seasonality factor (z) parameter*

181 The seasonality factor (z) parameter depends upon the local precipitation patterns such as the
182 hydrological characteristics of the area, its rainfall intensity and topography. In the InVEST water
183 yield model (Tallis et al. 2010), parameter z can be computed in three different ways. First method
184 is suggested by Donohue *et al.* (2012), in which parameter z is expressed as one fifth of the number
185 of rain events per year. Second method is suggested by Xu *et al.* (2013), which relates $w(x)$ with
186 latitude, NDVI (Normalized Difference Vegetation Index), area, etc. Third method experiments
187 with various selections of w (one value of w for the entire study region) till there is a good match
188 between observed and computed water yield. Unfortunately, this method is not suited for a pixel
189 based analysis as the number of pixels will be extremely large making the method to be
190 computationally intensive.

191 *2.1.2 Lumped Zhang model*

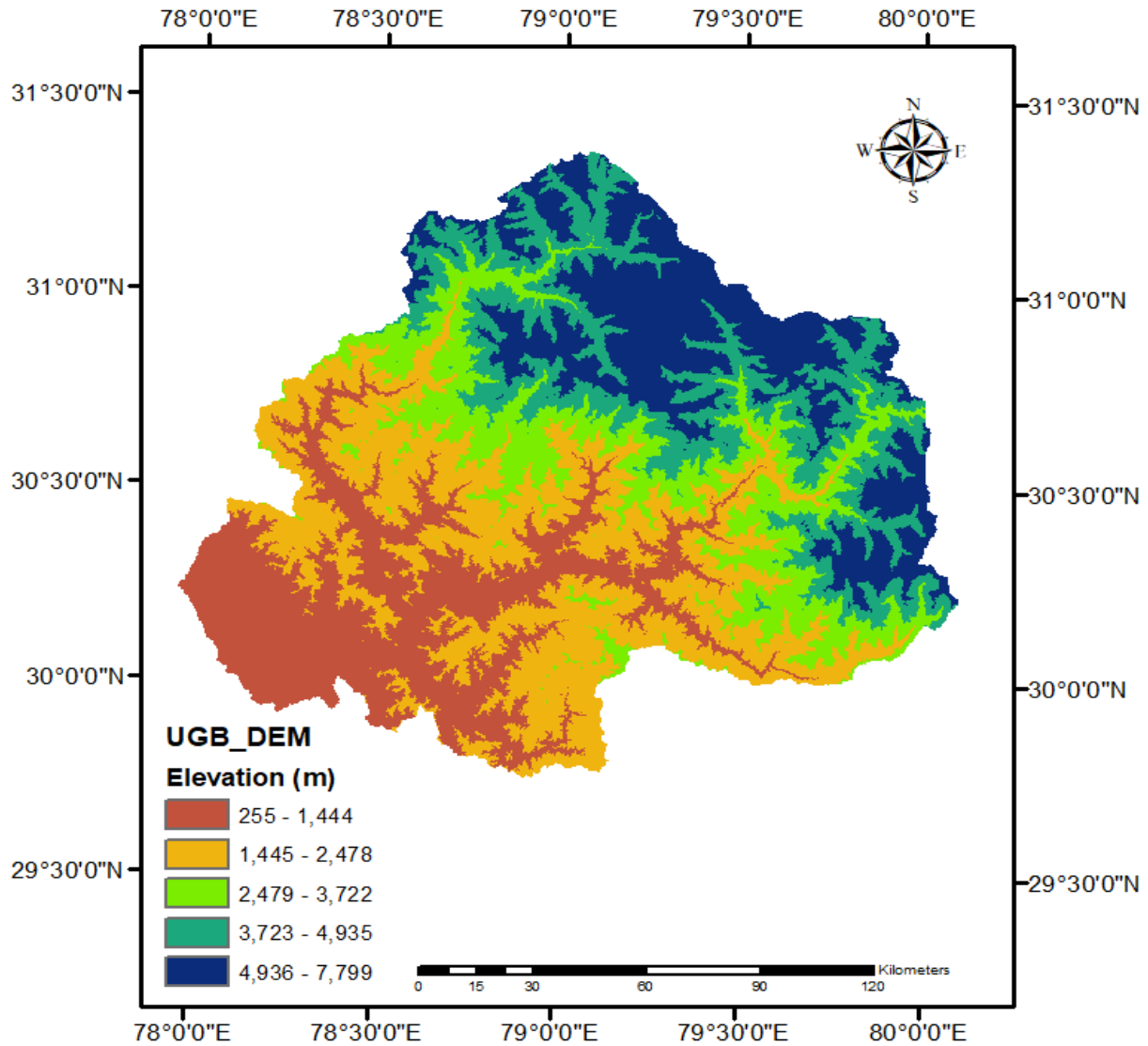
192 In this model, the mean value of the different parameters is used as an input to compute the average
193 value of the water yield for the whole watershed. The averaged actual evapotranspiration, potential
194 evapotranspiration, w , precipitation are described by Zhang *et al.* (2004).

195 **3. Study Area and Data**

196 *3.1 Study Area*

197 The Ganga river in India is ranked amongst the world's top 20 rivers in regards to the water
198 discharge. The Ganga river is segregated into three zones, viz., Upper Ganga basin, Middle Ganga

199 basin and Lower Ganga basin. The area chosen for the present study, i.e., Upper Ganga basin is
200 situated in the northern part of India within the geographical coordinates $30^{\circ} 38'$ - $31^{\circ} 24'$ N
201 latitude and $78^{\circ} 29'$ - $80^{\circ} 22'$ E longitude covering an area of 22,292.1 km² upto Haridwar. The
202 altitude of the study area varies from 7512 m in the Himalayan terrains to 275 m in the plains.
203 Approximately 433 km² of entire region of the basin is under glacier landscape and 288 km² is
204 under fluvial landscape. About 60% of the basin is utilized for agricultural, 20% of the basin is
205 under the forest area, especially in the upper mountainous region. Nearly 2% of the basin is
206 permanently covered with snow in the mountain peaks. Most predominant soil groups found in the
207 region are sand, clay, loam and their compositions. In the Upper Ganga river basin, the average
208 annual rainfall varies from 550 to 2500 mm (Bharati et al. 2011) where a major fraction of total
209 annual rainfall is received during monsoon months (June-September). The geographical location
210 and other information of the Upper Ganga river basin are represented in Fig. 1.



211

Figure 1. Graphical representation of study area, Upper Ganga basin

212

213 3.2 Data

214 3.2.1 Precipitation and Temperature

215 The daily time series of precipitation and temperature for the study area is acquired from India

216 Meteorological Department (IMD) at a grid size of 0.25 degrees and 1 degree, respectively. The

217 Upper Ganga basin comes in the latitude ranging from 29.5 degrees north to 31.5 degrees north

218 and longitude ranging from 77.75 degrees east to 80.25 degrees east. The daily time series of

219 precipitation was aggregated to obtain the annual time series at each grid point. Various analysis
220 in the study are carried out for four years i.e. 1980, 1990, 2001 and 2015.

221 *3.2.2 Soil Map*

222 Spatial maps of soil were collected from National Bureau of soil survey and land use planning
223 (NBSSLUP) at 1:250000. Digital maps of soil available at a resolution of 1200m×1200m were
224 resampled to the resolution of land use data i.e. 30m×30m using ‘resample’ tool in ArcGIS in order
225 to maintain the scale homogeneity. The attribute table of the raster layer contains fields like soil
226 depth, soil texture, percentage carbon content, drainage, slope, erosion, soil temperature and
227 mineralogy. The relevant feature, i.e. soil depth and soil texture are converted into the raster image
228 for the Upper ganga basin.

229 *3.2.3 LandUse/Land Cover map*

230 Satellite images were acquired from different sensors of Landsat viz. Landsat 3/4 MSS/TM,
231 Landsat 4 TM, Landsat 7 ETM and Landsat 8 OLI sensors for the year 1980, 1990, 2001 and
232 2015 respectively. The images are available at different resolution and for several bands out of
233 which Green (G), Red (R) and Near Infrared (NIR) band images are combined to create False
234 Colour Composite (FCC) for the study area in ERDAS Imagine. FCCs are then classified using
235 supervised classification in ERDAS in six different classes, i.e. Forest, Water, Agricultural,
236 Wasteland, Snow and Glacier and Built-up land. Classification of the area is based upon their
237 similar response under different bands. Each class is then recognized with the help of ground
238 truth and high resolution satellite images.

239 **4. Methodology**

240 In the present work, five different strategies are employed to compute water yield. For the ease of
 241 presentation, these strategies are referred as A, B, C, D and E. In strategy A, an average value of
 242 precipitation, temperature, extraterrestrial radiation and parameter ‘ w ’ is used for the entire basin.
 243 This strategy is essentially based on Lumped Zhang Model. Strategies B, C, D and E are designated
 244 corresponding to a particular variation of InVEST model where water yield is computed using
 245 different approach for estimating w parameter. For computing parameter ‘ w ’, Xu et al. (2013)
 246 relationship for large basin and global level is given by equation (9) and equation (10) respectively.

247 *For Large basins:*

$$248 \quad w = 0.69387 - 0.01042 \times lat + 2.81063 \times NDVI + 0.146186 \times CTI \quad (9)$$

249 *For global model:*

$$250 \quad w = 3.50412 - 0.09311 \times slp - 0.03288 \times lat + 1.12312 \times NDVI - 0.00205 \times long -$$

$$251 \quad 0.00026 \times elev \quad (10)$$

252 where, slp is slope gradient, lat is absolute latitude of basin center, CTI is compound topographic
 253 index, $NDVI$ is normalized difference vegetation index, $long$ is longitude and $elev$ is elevation.

254 In strategy B, entire basin is considered for computing the parameter w for large basins by Xu et
 255 al. (2013) (equation 9). In strategy C, entire basin is considered for computing the parameter w for
 256 global model (equation 10) by Xu et al. (2013). In strategy D, parameter w is computed at each
 257 pixel in order to incorporate the spatial distribution of the hydrologic variables involved in the
 258 computations. In Strategy E, parameter z is computed according to the number of rain events in a
 259 year and subsequently equation (4) is used to compute the parameter w .

260 For all the strategies, extraterrestrial radiation (RA) parameter is computed for each month using
261 equation (8) and a raster layer is generated. Precipitation data is obtained from Indian
262 Meteorological Department (IMD) at grid size of 0.25 degree for the study area. It has been
263 interpreted and converted to raster format by using Inverse Distance Weighted (IDW) interpolation
264 technique in ArcGIS environment for obtaining the values for all pixels at a resolution equal to the
265 resolution of the Landsat satellite images. The temperature dataset is obtained from IMD at grid
266 size of $1^{\circ} \times 1^{\circ}$ for the study area and has been interpreted and converted to raster format by using
267 IDW interpolation technique for obtaining the values for all pixels. Subsequently, the mean
268 monthly value of average temperature (T_{avg}) and the difference between mean daily maximum
269 and mean daily minimum (TD) is obtained. The climate datasets used in the present study are of
270 the finest resolution available so far for the study region. The precipitation and temperature data
271 sets were downscaled to a resolution of land use data using IDW interpolation technique. Gridded
272 datasets of temperature and precipitation used in the present study have been developed using
273 quality controlled stations and well-proven interpolation technique. Further details about the
274 datasets of precipitation and temperature are given in Srivastava et al. (2009) and Pai et al. (2014),
275 respectively.

276 Modified Hargreaves method is applied for obtaining the value of reference evapotranspiration at
277 each pixel for each month (Droogers et al. 2002). In this method, the inputs are RA, precipitation,
278 T_{avg} and TD. Some of the months, i.e. July 1980, July 1990, August 1990, June 2001, July 2001,
279 August 2001, June 2015, July 2015 and August 2015 showed negative values of reference
280 evapotranspiration as obtained from Modified Hargreaves method. For the above months, the
281 Hargreaves method as recommended by Droogers et al. (2002) is applied for obtaining the positive
282 values for the reference evapotranspiration. Thus, all the mean values for a month are added up to

283 get the mean yearly values for the year 1980, 1990, 2001 and 2015. To computed potential
 284 evapotranspiration, the yearly values obtained for the reference evapotranspiration have been
 285 multiplied by the vegetation evapotranspiration coefficient (K_c) which varies with the LULC
 286 characteristics as expressed in equation (3). The value of the K_c is taken from Allen *et al.* (1998)
 287 as shown in Table 1. In this study, K_c is taken same for all the four years as shown in Table. 1 and
 288 is used to obtain potential evapotranspiration which is subsequently used to obtain the annual water
 289 yield at each pixel of the study area.

290 **Table 1.** Value of K_c corresponding to LandUse/LandCover classes

S.No.	LandUse/LandCover	Percentage cover (1980)	Percentage cover (1990)	Percentage cover (2001)	Percentage cover (2015)	K_c
1	Forest	17.84	16.32	15.78	15.19	1
2	Water	21.87	21.27	19.47	17.65	1
3	Wastelands	51.1	52.36	54.18	55.46	0.2
4	Built-up Area	2.07	2.14	2.27	2.49	0.4
5	Agricultural	3.67	4.04	3.76	4.22	0.75
6	Snow and Glacier	3.45	3.87	4.54	4.99	2

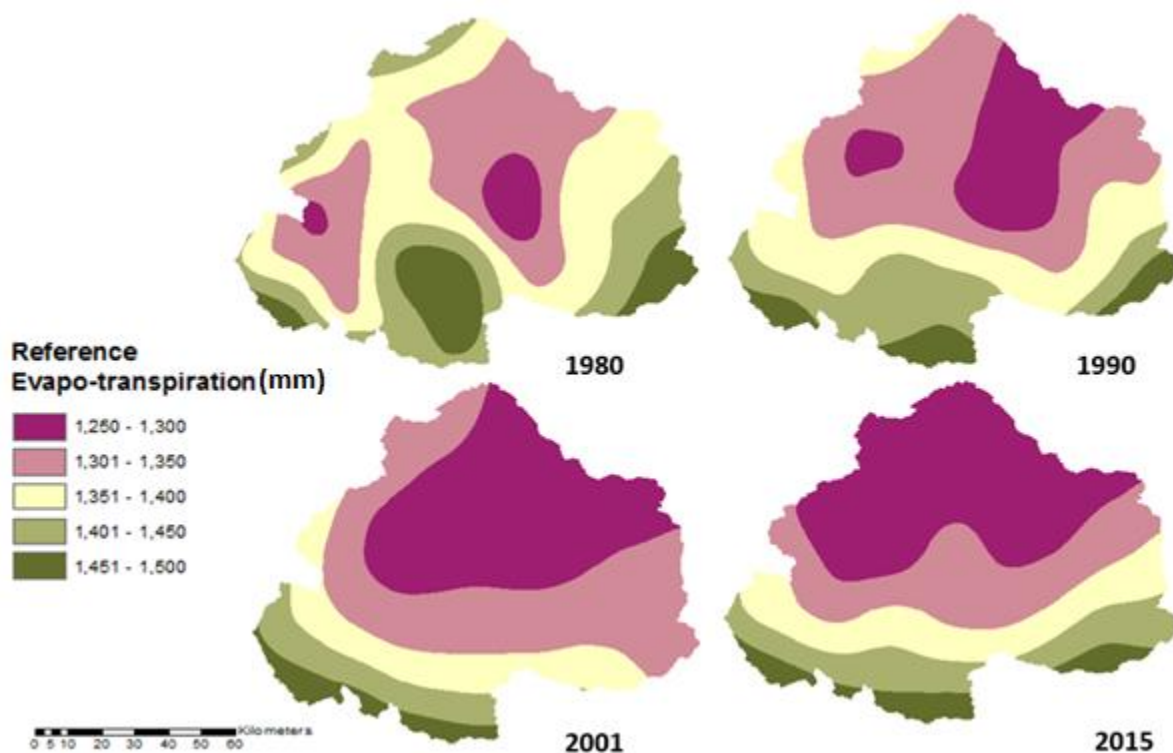
291

292 **5. Results**

293 **5.1 Reference Evapotranspiration, ET_0 (x)**

294 Reference Evapotranspiration (ET_0) is computed for the upper Ganga Basin using a high-
 295 resolution monthly climate dataset. Modified Hargreaves method is applied for obtaining the
 296 values of reference evapotranspiration at each pixel for each month (Droogers et al. 2002). ET_0 is

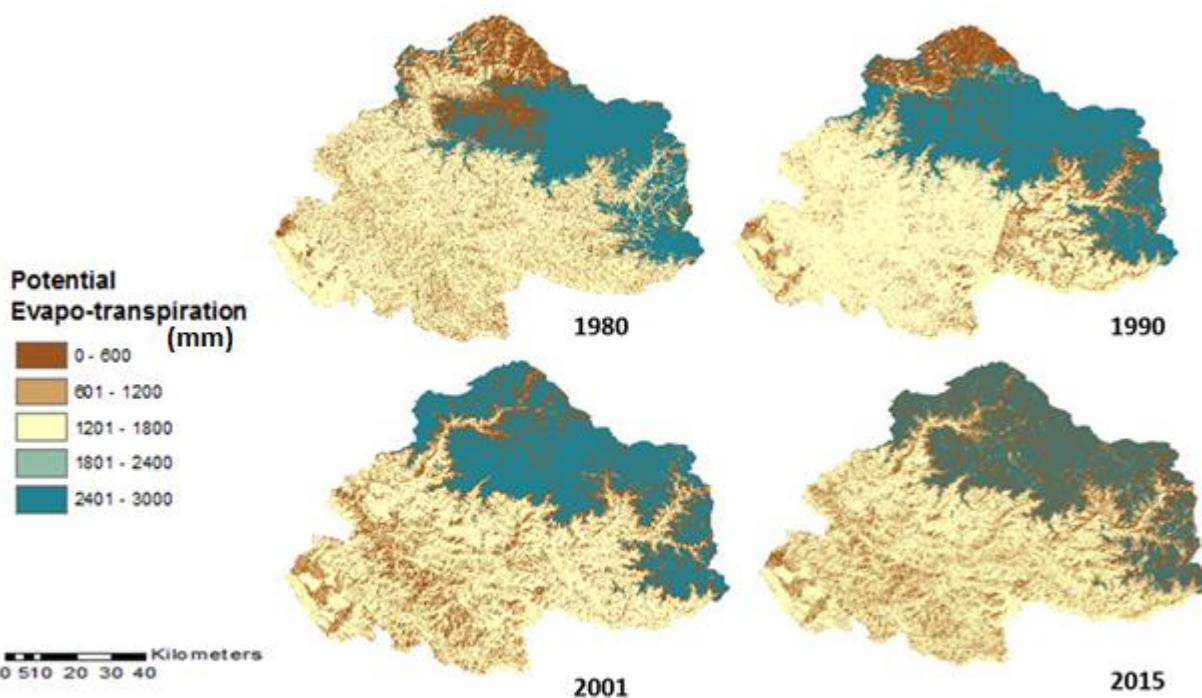
297 a function of RA, precipitation, Tavg and TD which are already computed pixel wise for each
298 month for the year 1980, 1990, 2001 and 2015. Some of the months i.e. July 1980, July 1990,
299 August 1990, June 2001, July 2001, August 2001, June 2015, July 2015 and August 2015 showed
300 negative values of reference evapotranspiration on applying Modified Hargreaves method. Thus,
301 for the above months, the Hargreaves method is applied for obtaining the positive results. Hence,
302 all the mean values for the months are added up to get the mean yearly values of evapotranspiration
303 for the years 1980, 1990, 2001 and 2015, as represented in Fig 2.



304
305 **Figure 2.** Reference Evapotranspiration (mm) of Upper Ganga Basin for the years 1980, 1990,
306 2001 and 2015.

307 **5.2 Potential Evapotranspiration, $PET(x)$**

308 The annual values obtained for the ET_0 is multiplied by the vegetation evapotranspiration
309 coefficient (K_c) which varies with the Land Use Land Cover characteristics, as expressed in
310 equation (3). The value of the K_c is taken from Allen et al. (1998). The values of the vegetation
311 evapotranspiration coefficient are taken from the Table 1. Thus, the potential evapotranspiration
312 is computed for Upper Ganga Basin for the years 1980, 1990, 2001 and 2015 as represented in
313 Fig. 3.



314
315 **Figure 3.** Potential Evapotranspiration (mm) of Upper Ganga Basin for the years 1980, 1990, 2001
316 and 2015.

317 *5.3 Water Yield, $Y(x)$*

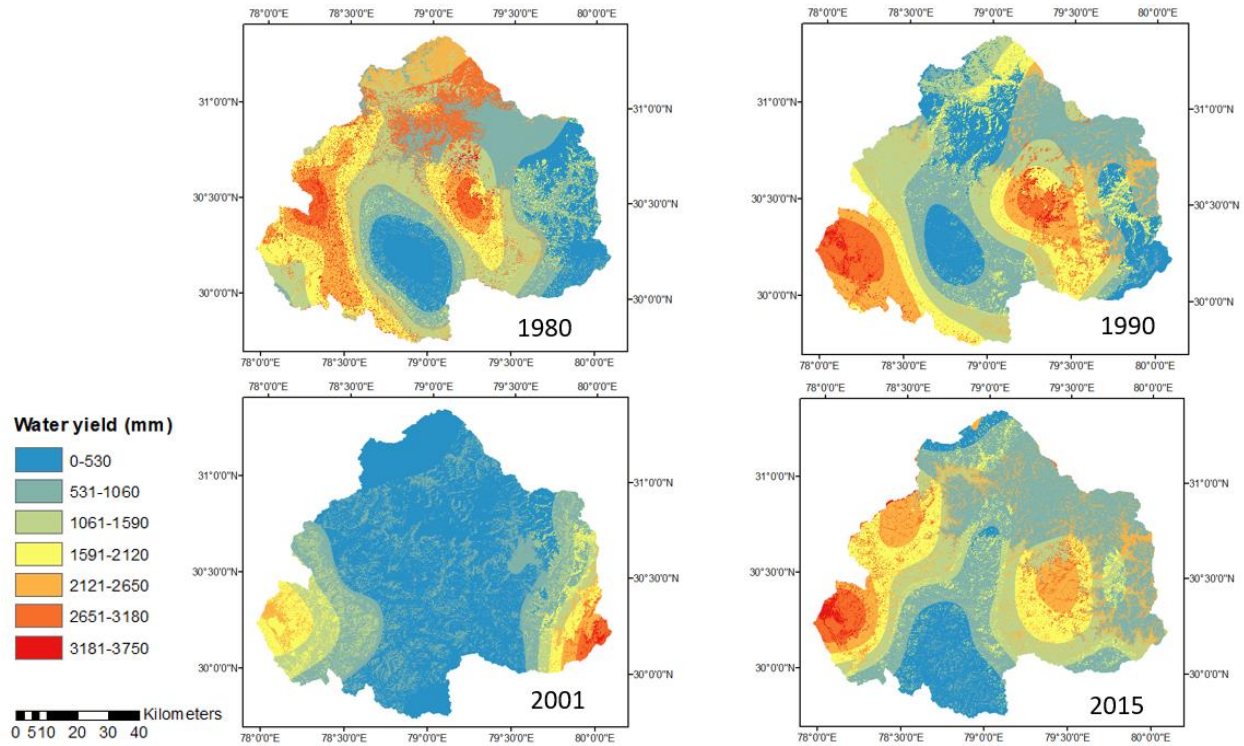
318 As mentioned in the methodology, the water yield for the Upper Ganga basin are computed using
319 five strategies namely A, B, C, D and E:

320 ***Strategy A: Water yield computed using Lumped Zhang Model***

321 Here, the basin average values of all the input parameters are considered and the water yield is
322 computed for the Upper Ganga basin for the year 1980, 1990, 2001 and 2015 which are obtained
323 as 658.52 mm, 925.68 mm, 603.71 mm and 1194.25 mm, respectively.

324 ***Strategy B: Water yield obtained by taking the single weighted mean value of parameter ‘w’***
325 ***from Xu et al. (2013) for Large basins.***

326 By considering a single value of the parameter w for the whole basin, the water yield is computed
327 for Upper Ganga basin (equation 9). The weighted mean value for the parameter w for the years
328 1980, 1990, 2001 and 2015 are obtained as 1.507, 1.541, 1.403 and 1.507, respectively. The spatial
329 distribution of water yield for the Upper Ganga basin for different years is represented in Fig. 4.
330 The mean values of water yield as obtained using this method for the year 1980, 1990, 2001 and
331 2015 are 755.65 mm, 959.48 mm, 742.39 mm and 1131.42 mm, respectively.

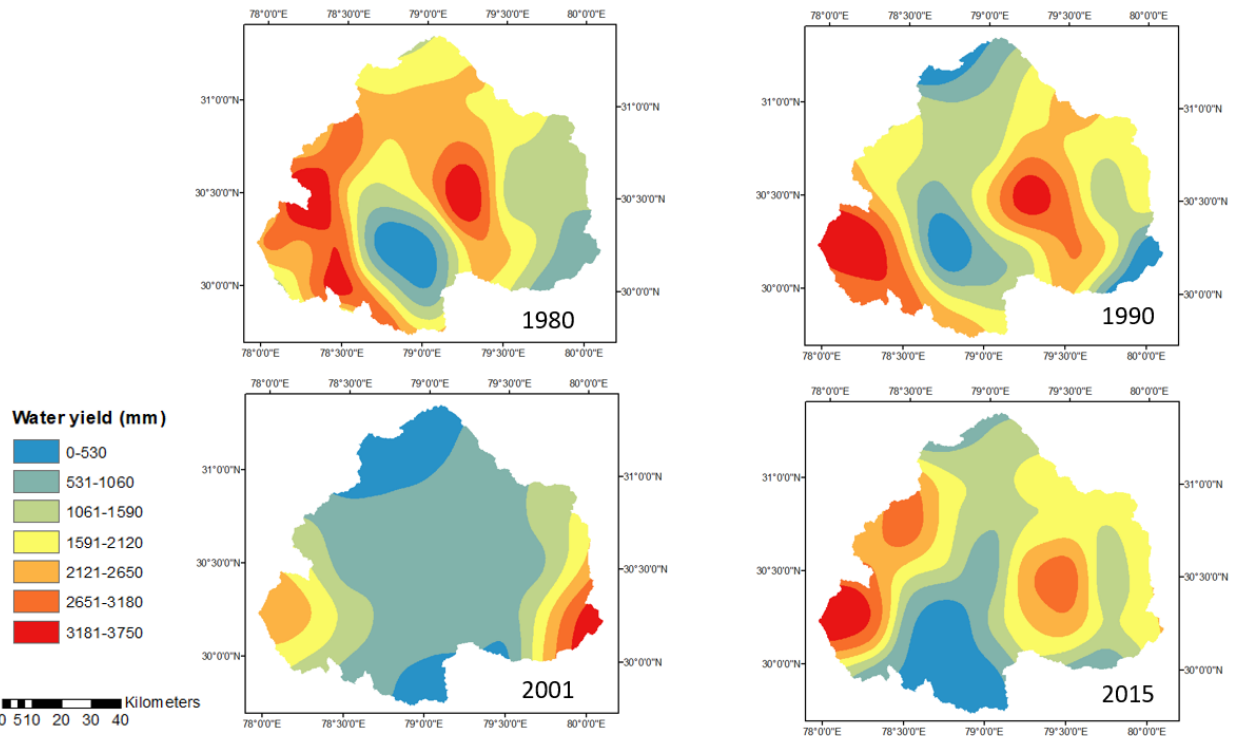


332

333 **Figure 4.** Water yield obtained by taking the single weighted mean value of parameter w from Xu
 334 et al. (2013) for large basins.

335 *Strategy C: Water yield obtained by taking the single weighted mean value of parameter ‘w’*
 336 *from Xu et al. (2013) for global model.*

337 In this strategy, water yield is computed by considering a single value of the parameter w for the
 338 entire Upper Ganga basin using equation 10. The weighted mean value for the parameter w for the
 339 years 1980, 1990, 2001 and 2015 are obtained as -0.967, -0.955, -1.010 and -0.968, respectively.
 340 The spatial distribution of water yield for the Upper Ganga basin for aforesaid years is shown in
 341 Fig. 5. The mean values of water yield for the year 1980, 1990, 2001 and 2015 are 1239.92 mm,
 342 1549.46 mm, 1149.93 mm and 1754.59 mm, respectively.

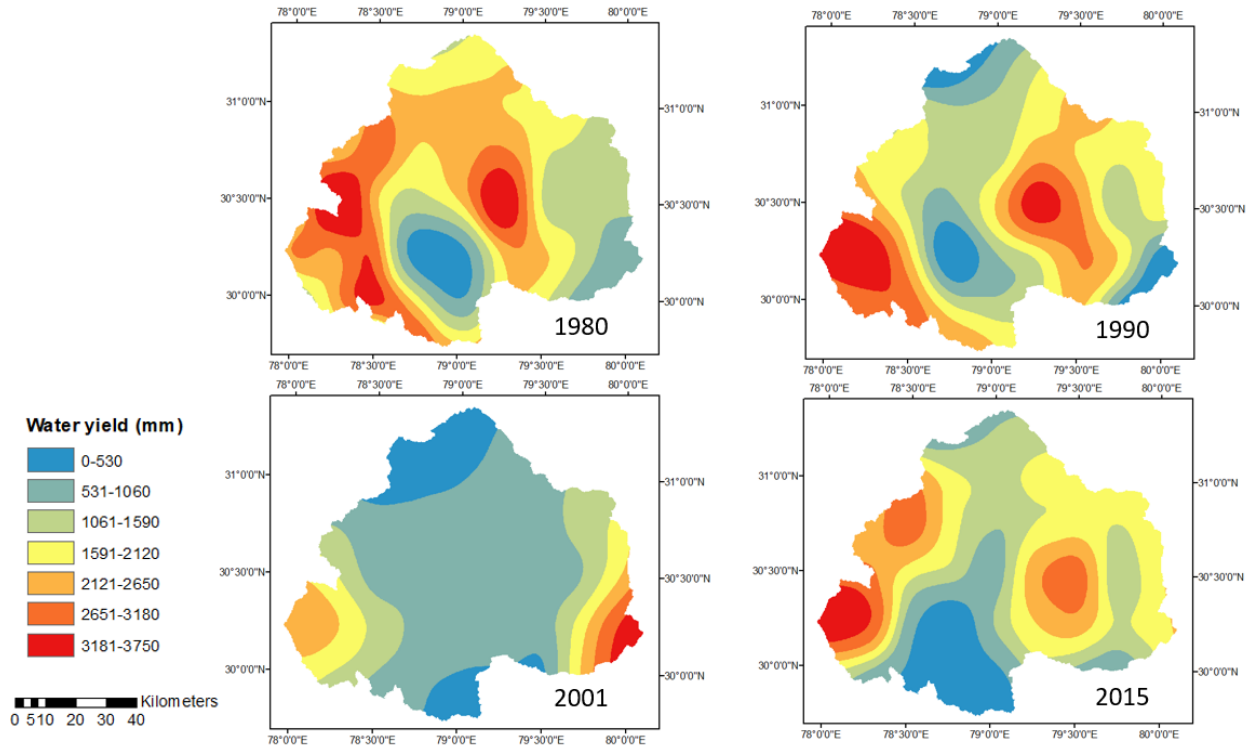


343

344 **Figure 5.** Water yield obtained by taking the single weighted mean value of parameter “w” from
 345 Xu et al. (2013) for global model.

346 *Strategy D: Water yield obtained using pixel level estimation of parameter ‘w’ from Xu et al.*
 347 *(2013)*

348 In this strategy, the values of parameter w are computed at pixel level. The water yield computed
 349 for the years 1980, 1990, 2001 and 2015 for the Upper Ganga Basin is shown in Fig. 6. The mean
 350 values of water yield for the year 1980, 1990, 2001 and 2015 are 1240.02 mm, 1549.44 mm,
 351 1149.89 mm and 1754.62 mm, respectively.

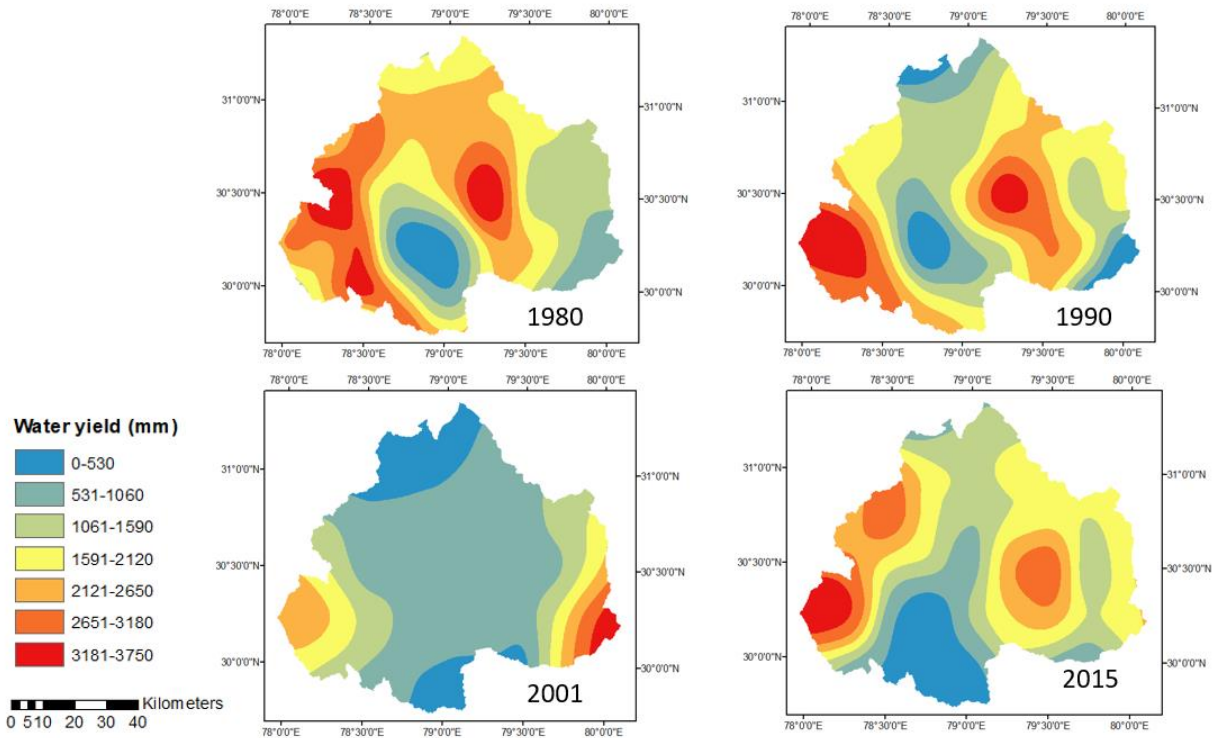


352

353 **Figure 6.** Water yield obtained by computing pixel wise value of parameter w from Xu et al.
 354 (2013)

355 *Strategy E: Water yield obtained using pixel level estimation of parameter ‘ w ’ from Donohue et*
 356 *al. (2012)*

357 Equation (4) represents the parameter w as a function of the parameters ‘ z ’, AWC and
 358 precipitation. The parameter w in the equation used in strategy ‘E’ has been proposed by Donohue
 359 et al. (2012) which is also cited in online documentation of InVEST model, however, the final
 360 equation used for estimating water yield is obtained from the InVEST model. Considering this
 361 fact, Donohue et al. (2012) has been cited in Strategy ‘E’. The water yield is computed for Upper
 362 Ganga Basin for different years is shown in Fig. 7. The mean values of water yield for the years
 363 1980, 1990, 2001 and 2015 are 1241.09 mm, 1552.38 mm, 1153.95 mm and 1753.53 mm,
 364 respectively.

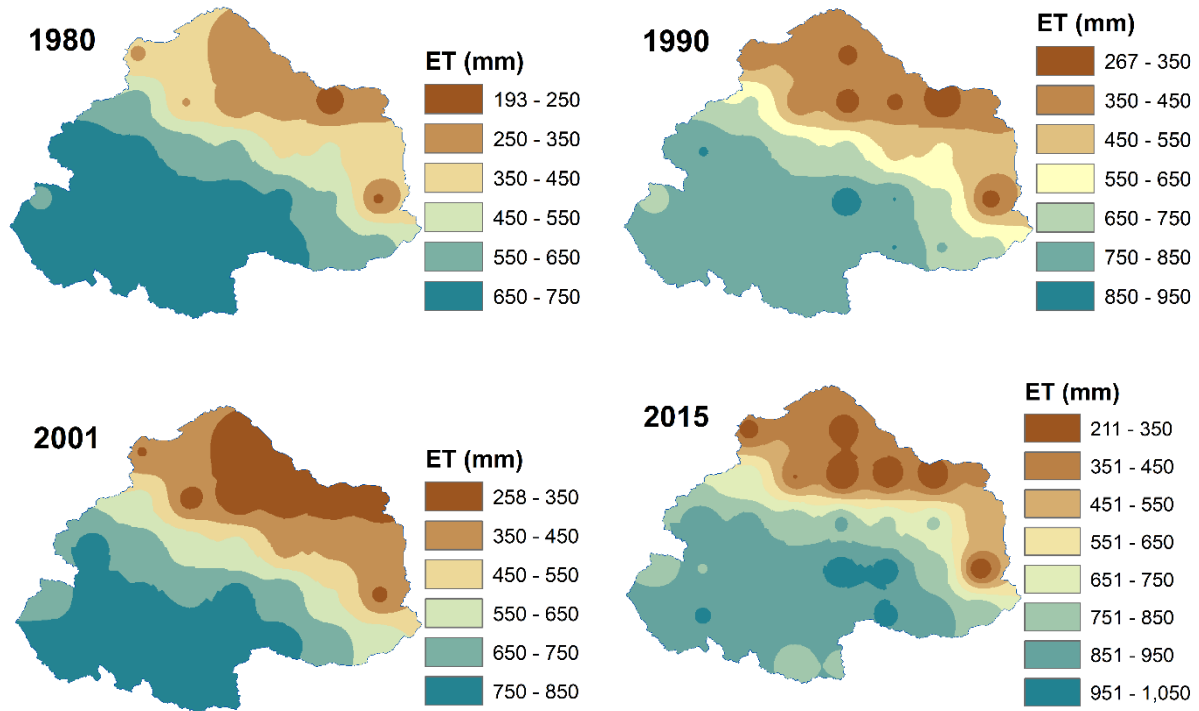


365

366 **Figure 7.** Water yield obtained by computing pixel wise value of parameter “w” from Donohue *et*
 367 *al.* (2012)

368 **5.2 Validation of ET and water yield estimates**

369 For validation purpose, the basin average annual values of PET and AET estimated using various
 370 strategies are compared with the corresponding basin average values obtained from available
 371 global datasets (Table 2). Model simulated AET values are obtained from GLDAS global ET
 372 datasets from Noah model outputs. Basin average values of PET dataset are obtained from Climate
 373 Research Unit (CRU) PET datasets (CRU TS v. 4.01) available at resolution of 0.5°. From the
 374 comparison, both AET (GLDAS) and PET (CRU TS) values are found to be in agreement with
 375 the satellite estimated values. Spatial maps of Global datasets of AET and PET are shown in Figure
 376 8 and 9, respectively.

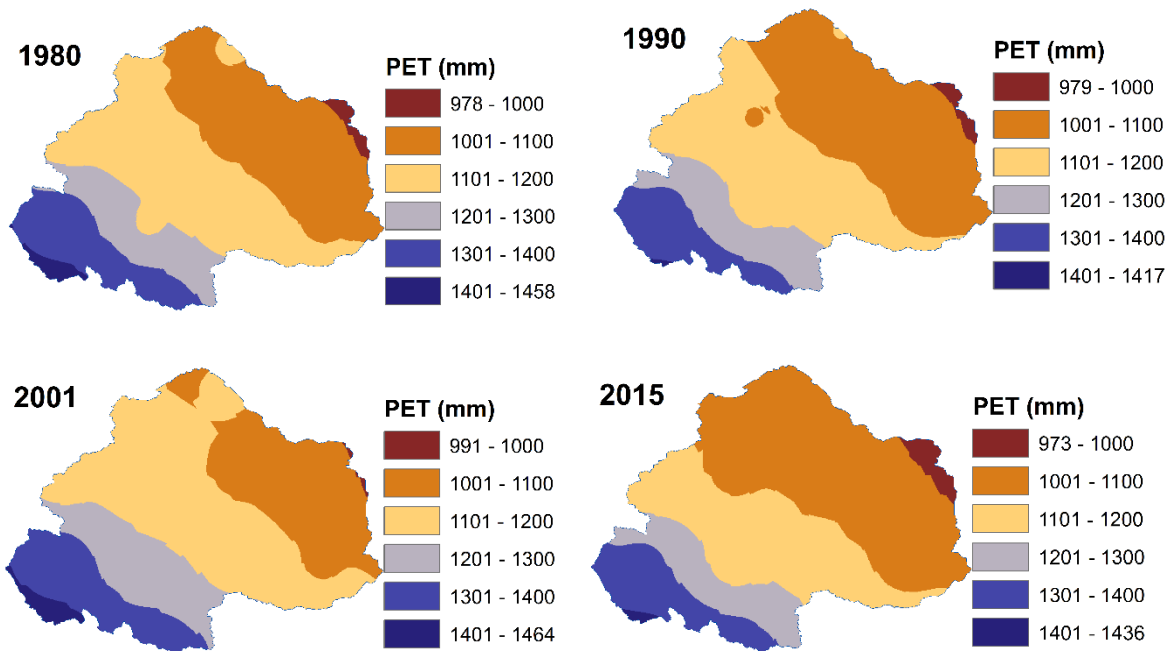


377

378

379 **Figure 8.** Spatial distribution of AET obtained from GLDAS Noah output datasets.

380



381

382

383 **Figure 9.** Spatial distribution of PET obtained from CRU datasets.

384

385

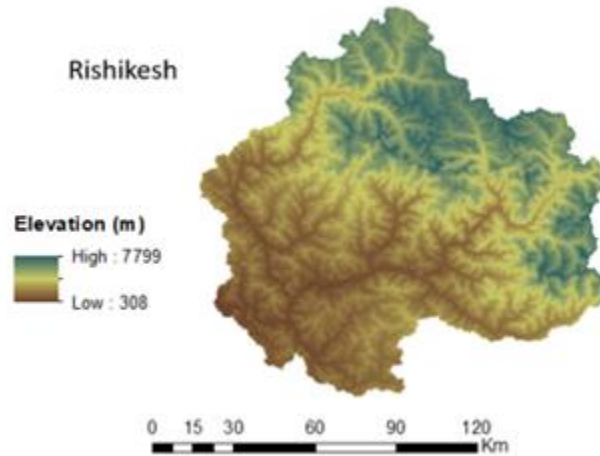
386
387

Table 2: Comparison of model estimated PET and AET with satellite estimates

Parameter (mm)	Year	Source 2 (GLDAS)	Source 2 (CRU)	InVEST model				
				Strategy A (Lumped Zhang Model)	Strategy B (Large Model)	Strategy C (Global model)	Strategy D (Xu et al. 2013)	Strategy E (Donohue et al. 2012)
AET	1980	555.0355		696.84	486.07	679.52	679.68	680.01
	1990	646.168		815.02	592.3	735.23	735.27	736.25
	2001	588.084		680.76	408.86	548.28	548.39	550.38
	2015	716.8316		900.11	625.41	743.48	743.52	744.34
PET	1980		1175.964	1376.64	1382.12	1382.12	1382.12	1382.12
	1990		1156.497	1456.16	1461.86	1461.86	1461.86	1461.86
	2001		1184.847	1457.08	1462.96	1462.96	1462.96	1462.96
	2015		1156.686	1544.20	1550.42	1550.42	1550.42	1550.42

388

389 The validation of water yield obtained from various strategies is performed upto Rishikesh gauging
 390 site of Upper Ganga basin (Fig. 10). The discharge data of the basin is obtained from Irrigation
 391 department of Uttarakhand state. Present work considers runoff from both precipitation as well as
 392 snowfall for the region, where 32% of the observed discharge has been removed as it is contributed
 393 by glacier ice melt as explained by Maurya et al. (2011) for our study area. The above mentioned
 394 fraction of discharge had been quantified using isotope study which separates the contribution of
 395 glacier melt in quantifying discharge (Maurya et al., 2011). A comparison of the water yield
 396 computed and observed for the study region for different years by various proposed strategies is
 397 shown in Table 3.



398

399

Figure 10. Graphical representation of sub-basin Rishikesh

400

Table 3. Observed vs computed water yield by various proposed strategies for Rishikesh sub-

401

basin.

Strategies	1980	1990	2001	2015
Observed discharge (mm)	1831.31	2422.43	2187.22	2835.81
Observed (mm) (after reducing approx. 32% snow melting contribution)	1245.29	1647.25	1487.31	1928.35
Water Yield_Strategy A (mm)	652.47	914.35	598.25	1189.72
Water Yield_Strategy B (mm)	745.38	917.77	697.75	1092.17
Water Yield_Strategy C (mm)	1229.90	1506.82	1102.62	1718.17
Water Yield_Strategy D (mm)	1229.99	1506.74	1102.61	1718.18
Water Yield_Strategy E (mm)	1230.77	1508.88	1106.86	1720.16

402

403

As can be seen in Table 3, values of water yield estimated using strategy A to E are systematically

404

increasing but are not steady in nature as water yield estimated using strategy A and B lies in range

405 650 – 750 mm whereas water yield from strategy C-E lies in range 1229 – 1231 mm for the year
406 1980 (see Table 3). Similar results are also evident for other years too. Also, water yield estimated
407 using strategy C-E are more or less same for a given year as these strategies involve pixel based
408 estimation of water yield considering spatial variation in Budyko parameters. The parameters
409 involved in Budyko model such as w are found to be dependent on various factors such as
410 catchment characteristics, vegetation cover, etc. as well as climate seasonality (Li et al. 2013). Ahn
411 and Merwade (2017) have analyzed the relationship between basin characteristics and parameter
412 w for 175 stations spread over the USA. Considering their study, no precise conclusion can be
413 drawn regarding relationship between basin characteristics and value of parameter w especially in
414 case of basin area characteristics. Moreover, no definite relationship has been yet identified
415 between basin characteristics and model parameters and is a subject matter for further study.

416 **6. Discussion**

417 The study aimed to apply the InVEST water yield model, a tool that is gaining interest in ecosystem
418 services community for Upper Ganga Basin having highly variable topography consisting of hilly
419 areas, plain areas and the regions which are totally covered with snow. The InVEST model is based
420 upon Budyko theory which requires low amount of data and low level of expertise, thus making it
421 acceptable world-wide. Monthly precipitation, monthly average value of temperature, monthly
422 value of difference of mean daily maximum and mean daily minimum and extraterrestrial radiation
423 parameters for the Upper Ganga Basin for each month of all the four years i.e. 1980, 1990, 2001
424 and 2015 are converted into raster format for various analysis. The monthly reference
425 evapotranspiration is thus computed using input parameters in GIS environment by applying the
426 modified Hargreaves equation for all the months except some months where the modified
427 Hargreaves equation shows the negative results for the reference evapotranspiration value. For

428 those months, Hargreaves method is applied to obtain the positive value of reference
429 evapotranspiration as also suggested by Goyal et al. (2017). Reference evapotranspiration when
430 multiplied with K_c gives the potential evapotranspiration. All monthly values are added up to
431 obtain the annual value of reference evapotranspiration. K_c is a function of Land Use Land Cover,
432 thus, supervised classification is done to prepare the raster Land Use Land Cover map for the
433 Upper Ganga Basin. Subsequently, the annual value of potential evapotranspiration is obtained for
434 the study area for the years 1980, 1990, 2001 and 2015.

435 The paper focuses on various methodologies used for water yield estimation as discussed in the
436 paper and is applied on the Upper Ganga basin. Thus, water yield is computed both from InVEST
437 model as well as Lumped Zhang model. The value of the parameter w is computed using four
438 ways, i.e. mean single value obtained from Xu et al. (2013) for large basins and global model,
439 pixel wise value of parameter w from Xu et al. (2013) and pixel wise value of parameter w from
440 Donohue et al. (2012). Although, the Upper Ganga basin lies in large basin category as per the
441 definition from Xu et al. (2013), but, the yield computed using global model is in good agreement
442 with the observed data for the Upper Ganga basin. In the study, pixel level estimation of parameter
443 w is made in order to incorporate the spatial variability of the parameter in water yield estimation.
444 Thus, two pixel wise values of parameter w are computed for the Upper Ganga basin for years
445 1980, 1990, 2001 and 2015 by considering two approaches as given by Xu et al. (2013) and
446 Donohue et al. (2012). Also, the water yield is computed from Lumped Zhang model which works
447 on the approach of considering mean values of all the parameters involved in the computation of
448 water yield. Thus, water yield is computed in five different ways for the Upper Ganga basin for
449 the years 1980, 1990, 2001 and 2015.

450 At Rishikesh gauging site, surface runoff data is obtained by extracting the snow melt from the
451 discharge data as the snow melting contributes about 32 percent of total runoff (Maurya et al.,
452 2011). Using this fact, the observed yield is compared with the computed water yield based on
453 different proposed strategies for the years 1980, 1990, 2001 and 2015 as represented in Table 3.
454 The results obtained from Donohue et al. (2012) and Xu et al. (2013) are computed at pixel level
455 (Strategy C, Strategy D and Strategy E), thus, exhibit better performance than other approaches
456 and are in good agreement with the observed data. It is clear that in order to go for hydrological
457 analysis for any watershed, pixel wise computation is advisable. The parameters involved in the
458 Budyko model are dependent on various factors such as basin characteristics (size, topography,
459 stream length, slope, etc.), climate seasonality, etc. (Li et al., 2013). The factors affecting model
460 parameters again vary both spatially and temporally. Moreover, the relationship between these
461 factors and model parameters are not yet well defined (Ahn and Merwade, 2017). In such scenario,
462 adopting a hypothesis by assuming either of these controlling factors (such as 'w') to be constant
463 spatially or temporally is inappropriate. Considering these facts, the present study attempts to
464 incorporate the spatial variability of model parameter for estimation of water yield at pixel level.
465 As the computations are made at pixel level in GIS environment, the assumption of dependence
466 of model parameters over scale of the catchment may also be disregarded. The computations made
467 in present work are based on empirical equations, however, the application of these equations has
468 been well documented worldwide for estimation of various water balance components at various
469 basin scales (Zhang et al., 2008; Ma et al., 2008; Ning et al., 2017; Rouholahnejad et al., 2017;
470 Wang et al., 2017). Hence, it is recommended that for such a large basin there is a strong need to
471 compute all the parameters involved in the computations of water yield at pixel scale rather than
472 adopting mean values for entire watershed.

473 **7. Summary and Conclusions**

474 The present study aimed to apply the InVEST annual water yield model, a tool that is gaining
475 interest in the ecosystem services community. While such simple models having low requirements
476 for data, high level of expertise are needed for practical applications of such model as a single
477 representative value of model parameter for the entire basin does not provide accurate estimates
478 of water yield. In addition, performing pixel scale computation of water yield indicates a better
479 performance and results obtained show better agreement with the observed water yield. As far as
480 parameter w is concerned, global model works better than other representations of parameter w
481 available in literature. In the study, the water yield is computed using five different strategies and
482 results are analyzed with the observed data at the outlet of Upper Ganga Basin. The present study
483 attempts to quantify annual water yield at pixel level making the computations independent of the
484 size of catchment. Therefore, the proposed methodology is expected to perform well for the
485 catchment of any given size. Changes in catchment water storage over time are required to be
486 quantified in order to validate the applicability of Budyko's model to long term data for the
487 catchment under study. Earlier, some of the important parameters for the water yield used to be
488 computed at a basin level scale which brings noise in the results. Thus, by considering all the
489 parameters involved in the model at pixel level scale, the results obtained are higher in accuracy.

490 The study attempts to incorporate the spatial variability of parameters involved in the model
491 thorough pixel level estimation of parameters which are otherwise taken as lumped in the previous
492 studies. Study results show that the water yield estimated considering spatial variability in model
493 parameters are in better agreement with the observed water yield as compared to the water yield
494 estimated by considering the parameters to be lumped over the study region. Further, the
495 computations of various parameters are made at pixel level, therefore, the estimates of water

496 balance components using this approach are expected to be independent of the assumption of
497 dependence of parameters on catchment size. As the variation between Budyko's model
498 parameters and their controlling factors has not shown well defined relationship (Ahn and
499 Merwade, 2017), the study emphasizes water yield estimation using pixel based computations.
500 Therefore, it can be inferred that: (i) between two approaches used, i.e. considering entire basin
501 and pixel level approach, the pixel level approach is found to provide better results and (ii) in pixel
502 based computations, results are further improved with the use of a parameter w based on a global
503 model rather than regional models of parameter w for large basins in Himalayan region.

504 **Acknowledgement**

505 Authors are thankful to Executive Engineer, Irrigation Department, Uttarakhand, for providing the
506 discharge data for the Rishikesh sub-basin of Upper Ganga Basin.

507 **References**

508 Ahn, K. H., and Merwade, V. (2017). "The Integrated Impact of Basin Characteristics on Changes
509 in Hydrological Variables", Book Chapter 12 in "*Sustainable Water Resources Management*",
510 American Society of Civil Engineers (ASCE), pp. 317-336. ISBN: 978-0-7844-1476-7.

511 Allen, R. G., Pereira, L. S., Raes, D., and Smith, M. (1998). "Crop evapotranspiration-Guidelines
512 for computing crop water requirements"-FAO Irrigation and drainage paper 56. FAO, Rome,
513 300(9), D05109.

514 Bai, Y., Ouyang, Y., and Pang, J. S. (2012). "Biofuel supply chain design under competitive
515 agricultural land use and feedstock market equilibrium." *Energy Economics*, 34(5), 1623-1633.

516 Berghuijs, W. R., Woods, R. A., and Hrachowitz, M. (2014). “A precipitation shift from snow
517 towards rain leads to a decrease in streamflow.” *Nature Climate Change*, 4(7), 583-586.

518 Bharati, Luna, Guillaume Lacombe, Pabitra Gurung, Priyantha Jayakody, Chu Thai Hoanh, and
519 Vladimir Smakhtin (2011). *The impacts of water infrastructure and climate change on the*
520 *hydrology of the Upper Ganges River Basin*. Vol. 142. IWMI, 2011.

521 Budyko, M. (1958). *The Heat Balance of the Earth, Leningrad, 1956* (in Russian), Translation by
522 N. A. Stepanova, US Weather Bureau, Washington, p. 255.

523 Budyko, M. I. (1974). *Climate and Life*, Academic Press, New York, USA, 1-507.

524 Budyko, M. I., and Ronov, A. B. (1979). “Evolution of chemical composition of the atmosphere
525 during the Phanerozoic.” *Geokhimiya*, (5), 643-653.

526 Burkhard, B., Crossman, N., Nedkov, S., Petz, K., and Alkemade, R. (2013). “*Mapping and*
527 *modelling ecosystem services for science, policy and practice*. (4), 1-3.

528 Chen, X., Alimohammadi, N., and Wang, D. (2013). “Modeling interannual variability of seasonal
529 evaporation and storage change based on the extended Budyko framework.” *Water Resources*
530 *Research*, 49(9), 6067-6078.

531 Choudhury, B. (1999). “Evaluation of an empirical equation for annual evaporation using field
532 observations and results from a biophysical model.” *Journal of Hydrology*, 216(1), 99-110.

533 Donohue, R. J., Roderick, M. L., and McVicar, T. R. (2006). “On the importance of including
534 vegetation dynamics in Budyko’s hydrological model.” *Hydrology and Earth System Sciences*
535 *Discussions*, 3(4), 1517-1551.

536 Donohue, R. J., Roderick, M. L., and McVicar, T. R. (2012). "Roots, storms and soil pores:
537 Incorporating key ecohydrological processes into Budyko's hydrological model." *Journal of*
538 *Hydrology*, 436, 35-50.

539 Droogers, P., and Allen, R. G. (2002). "Estimating reference evapotranspiration under inaccurate
540 data conditions." *Irrigation and drainage systems*, 16(1), 33-45.

541 Fu, B. P. (1981). "On the calculation of the evaporation from land surface." *Sci. Atmos. Sin*, 5(1),
542 23-31.

543 Gentine, P., D'Odorico, P., Lintner, B. R., Sivandran, G., and Salvucci, G. (2012).
544 "Interdependence of climate, soil, and vegetation as constrained by the Budyko curve."
545 *Geophysical Research Letters*, 39(19), L19404.

546 Goyal, M. K., and Khan, M. (2017). "Assessment of spatially explicit annual water-balance model
547 for Sutlej River Basin in eastern Himalayas and Tungabhadra River Basin in peninsular India."
548 *Hydrology Research*, 48(2), 542-558.

549 Guswa, A. J., Brauman, K. A., Brown, C., Hamel, P., Keeler, B. L., and Sayre, S. S. (2014).
550 "Ecosystem services: Challenges and opportunities for hydrologic modeling to support decision
551 making." *Water Resources Research*, 50(5), 4535-4544.

552 Hamel, P., and Guswa, A. J. (2014). "Uncertainty analysis of a spatially-explicit annual water-
553 balance model: case study of the Cape Fear catchment, NC." *Hydrology and Earth System*
554 *Sciences*, 11, 11001-11036.

555 Hoyer, R., and Chang, H. (2014). "Assessment of freshwater ecosystem services in the Tualatin
556 and Yamhill basins under climate change and urbanization." *Applied Geography*, 53, 402-416.

557 Khatami, S., and Khazaei, B. (2014). “Benefits of GIS Application in Hydrological Modeling: A
558 Brief summary.” *VATTEN–Journal of Water Management and Research*, 70, 41-49.

559 Li, D., Pan, M., Cong, Z., Zhang, L., and Wood, E. (2013). “Vegetation control on water and
560 energy balance within the Budyko framework.” *Water Resources Research*, 49(2), 969-976.

561 Liston, G. E., and Elder, K. (2006). “A distributed snow-evolution modeling system
562 (SnowModel).” *Journal of Hydrometeorology*, 7(6), 1259-1276.

563 Ma, Z. M., S. Z. Kang, L. Zhang, L. Tong, and X. L. Su (2008). “Analysis of impacts of climate
564 variability and human activity on streamflow for a river basin in arid region of northwest China.”
565 *Journal of Hydrology*, 352(3–4), 239–249.

566 Maurya, A. S., Shah, M., Deshpande, R. D., Bhardwaj, R. M., Prasad, A., and Gupta, S. K. (2011).
567 “Hydrograph separation and precipitation source identification using stable water isotopes and
568 conductivity: River Ganga at Himalayan foothills.” *Hydrological Processes*, 25(10), 1521-1530.

569 McKenzie, N. J., Gallant, J., and Gregory, L. (2003). “*Estimating water storage capacities in soil*
570 *at catchment scales.*” CRC for Catchment Hydrology.

571 Mezentsev, V. (1955). “More on the computation of total evaporation (Yechio raz o rastchetie
572 srednevo summarnovo ispareniiia)” *Meteorog. i Gridrolog.*, 5, 24–26, 1955.

573 Milly, P. C. D. (1994). “Climate, soil water storage, and the average annual water balance.” *Water*
574 *Resources Research*, 30(7), 2143-2156.

575 Milly, P. C. D., and Dunne, K. A. (2002). “Macroscale water fluxes 2. Water and energy supply
576 control of their interannual variability.” *Water Resources Research*, 38(10), 241-249.

577 Nelson, E., Sander, H., Hawthorne, P., Conte, M., Ennaanay, D., Wolny, S., ... and Polasky, S.
578 (2010). “Projecting global land-use change and its effect on ecosystem service provision and
579 biodiversity with simple models.” *PloS one*, 5(12), E14327.

580 Ning, T., Li, Z., and Liu, W. (2017). “Vegetation dynamics and climate seasonality jointly control
581 the interannual catchment water balance in the Loess Plateau under the Budyko framework.”
582 *Hydrology and Earth System Sciences*, 21, 1515-1526

583 Ojha C.S.P., Bhunya P., and Berndtsson R. (2008). *Engineering Hydrology*, 1st Ed., Oxford
584 University Press, UK, 1-459.

585 Ol’Dekop, E. M. (1911). *On Evaporation from the Surface of River Basins*, Univ. of Tartu, Tartu,
586 Estonia, p. 209.

587 Pai, D. S., Sridhar, L., Rajeevan, M., Sreejith, O. P., Satbhai, N. S., and Mukhopadhyay, B. (2014).
588 “Development of a new high spatial resolution (0.25× 0.25) long period (1901–2010) daily gridded
589 rainfall data set over India and its comparison with existing data sets over the region.” *Mausam*,
590 65(1), 1-18.

591 Pathak, S., Ojha, C. S. P., Zevenbergen, C., and Garg, R. D. (2017). “Ranking of Storm Water
592 Harvesting Sites Using Heuristic and Non-Heuristic Weighing Approaches.” *Water*, 9(9), 710.

593 Pike, J. G. (1964). “The estimation of annual run-off from meteorological data in a tropical
594 climate.” *Journal of Hydrology*, 2(2), 116-123.

595 Porporato, A., Daly, E., and Rodriguez-Iturbe, I. (2004). “Soil water balance and ecosystem
596 response to climate change.” *The American Naturalist*, 164(5), 625-632.

597 Potter, N. J., Zhang, L., Milly, P. C. D., McMahon, T. A., and Jakeman, A. J. (2005). “Effects of
598 rainfall seasonality and soil moisture capacity on mean annual water balance for Australian
599 catchments.” *Water Resources Research*, 41(6), 1-11.

600 Rouholahnejad Freund, E. and Kirchner, J. W. (2017). “A Budyko framework for estimating how
601 spatial heterogeneity and lateral moisture redistribution affect average evapotranspiration rates as
602 seen from the atmosphere.” *Hydrology and Earth System Sciences*, 21, 217-233

603 Sánchez-Canales, M., Benito, A. L., Passuello, A., Terrado, M., Ziv, G., Acuña, V., ... and Elorza,
604 F. J. (2012). “Sensitivity analysis of ecosystem service valuation in a Mediterranean watershed.”
605 *Science of the total environment*, 440, 140-153.

606 Schreiber, P. (1904). “Über die Beziehungen zwischen dem Niederschlag und der Wasserführung
607 der Flüsse in Mitteleuropa.” *Z. Meteorol*, 21(10), 441-452.

608 Shao, Q., Traylen, A., and Zhang, L. (2012). “Nonparametric method for estimating the effects of
609 climatic and catchment characteristics on mean annual evapotranspiration.” *Water Resources
610 Research*, 48(3), W03517.

611 Srivastava, A. K., Rajeevan, M., and Kshirsagar, S. R. (2009). “Development of a high resolution
612 daily gridded temperature data set (1969–2005) for the Indian region.” *Atmospheric Science
613 Letters*, 10(4), 249-254.

614 Su, C., and Fu, B. (2013). “Evolution of ecosystem services in the Chinese Loess Plateau under
615 climatic and land use changes.” *Global and Planetary Change*, 101, 119-128.

616 Tallis, H.T., Ricketts, T., Nelson, E., Ennaanay, D., Wolny, S., Olwero, N., Vigerstol, K.,
617 Pennington, D., Mendoza, G., Aukema, J. and Foster, J., (2010). *InVEST 1.004 beta User's Guide*.
618 The Natural Capital Project.

619 Terrado, M., Acuña, V., Ennaanay, D., Tallis, H., and Sabater, S. (2014). “Impact of climate
620 extremes on hydrological ecosystem services in a heavily humanized Mediterranean basin.”
621 *Ecological Indicators*, 37, 199-209.

622 Turc, L. (1954). “Le bilan d’eau des sols: relations entre les précipitations, l’évaporation et
623 l’écoulement.” *Annales Agronomiques A*, 20, 491–595.

624 Wang, D., and Tang, Y. (2014). “A one-parameter Budyko model for water balance captures
625 emergent behavior in darwinian hydrologic models.” *Geophysical Research Letters*, 41(13), 4569-
626 4577.

627 Wang, X.-S. and Zhou, Y. (2017). “Shift of annual water balance in the Budyko space for
628 catchments with groundwater-dependent evapotranspiration.” *Hydrology and Earth System
629 Sciences*, 20, 3673-3690

630 Williams, C. A., Reichstein, M., Buchmann, N., Baldocchi, D., Beer, C., Schwalm, C., ... and
631 Papale, D. (2012). “Climate and vegetation controls on the surface water balance: Synthesis of
632 evapotranspiration measured across a global network of flux towers.” *Water Resources Research*,
633 48(6), W06523.

634 Xu, X., Liu, W., Scanlon, B. R., Zhang, L., and Pan, M. (2013). “Local and global factors
635 controlling water-energy balances within the Budyko framework.” *Geophysical Research Letters*,
636 40(23), 6123-6129.

637 Yang, D., Sun, F., Liu, Z., Cong, Z., Ni, G., and Lei, Z. (2007). “Analyzing spatial and temporal
638 variability of annual water-energy balance in nonhumid regions of China using the Budyko
639 hypothesis.” *Water Resources Research*, 43(4), W04426.

640 Yang, H., Yang, D., Lei, Z., and Sun, F. (2008). “New analytical derivation of the mean annual
641 water-energy balance equation.” *Water Resources Research*, 44(3), W03410.

642 Zhang, L., Dawes, W. R., and Walker, G. R. (2001). “Response of mean annual evapotranspiration
643 to vegetation changes at catchment scale.” *Water resources research*, 37(3), 701-708.

644 Zhang, L., Hickel, K., Dawes, W. R., Chiew, F. H., Western, A. W., and Briggs, P. R. (2004). “A
645 rational function approach for estimating mean annual evapotranspiration.” *Water Resources
646 Research*, 40(2), W02502.

647 Zhang, L., N. Potter, K. Hickel, Y. Q. Zhang, and Q. X. Shao (2008). “Water balance modeling
648 over variable time scales based on the Budyko framework—Model development and testing.”
649 *Journal of Hydrology*, 360(1–4), 117–131.

650 Zhou, G., Wei, X., Chen, X., Zhou, P., Liu, X., Xiao, Y., ... and Su, Y. (2015). “Global pattern for
651 the effect of climate and land cover on water yield.” *Nature communications*, 6, 5918.

652 Zhou, S., Yu, B., Huang, Y., and Wang, G. (2015). “The complementary relationship and
653 generation of the Budyko functions.” *Geophysical Research Letters*, 42(6), 1781-1790.

654 Zhou, X., Zhang, Y., Wang, Y., Zhang, H., Vaze, J., Zhang, L., ... and Zhou, Y. (2012).
655 “Benchmarking global land surface models against the observed mean annual runoff from 150
656 large basins.” *Journal of Hydrology*, 470, 269-279.

657